Title

Intramyocardial injection of hydrogel with high interstitial spread does not impact action potential propagation

Authors

Suarez, Sophia L
Rane, Aboli A
Muñoz, Adam
et al.

Publication Date

2015-10-01

DOI

10.1016/j.actbio.2015.08.004

Peer reviewed

HHS Public Access

Author manuscript

Acta Biomater. Author manuscript; available in PMC 2016 October 15.

Published in final edited form as:

Acta Biomater. 2015 October 15; 26: 13–22. doi:10.1016/j.actbio.2015.08.004.

Intramyocardial injection of hydrogel with high interstitial spread does not impact action potential propagation

Sophia L. Suarez[a,b,c], **Aboli A. Rane**[a,b], **Adam Muñoz**[a,b], **Adam T. Wright**[a], **Shirley X. Zhang**[a,b], **Rebecca L. Braden**[a,b], **Adah Almutairi**[c,*], **Andrew D. McCulloch**[a], and **Karen L. Christman**[a,b,*]

[a]Department of Bioengineering, University of California, San Diego, La Jolla, CA 92093, USA

[b]Sanford Consortium for Regenerative Medicine, University of California, San Diego, La Jolla, CA 92037, USA

[c]Skaggs School of Pharmacy and Pharmaceutical Sciences, University of California at San Diego, La Jolla, California 92093, USA

Abstract

Injectable biomaterials have been evaluated as potential new therapies for myocardial infarction (MI) and heart failure. These materials have improved left ventricular (LV) geometry and ejection fraction, yet there remain concerns that biomaterial injection may create a substrate for arrhythmia. Since studies of this risk are lacking, we utilized optical mapping to assess the effects of biomaterial injection and interstitial spread on cardiac electrophysiology. Healthy and infarcted rat hearts were injected with a model poly(ethylene glycol) hydrogel with varying degrees of interstitial spread. Activation maps demonstrated delayed propagation of action potentials across the LV epicardium in the hydrogel-injected group when compared to saline and no-injection groups. However, the degree of the electrophysiological changes depended on the spread characteristics of the hydrogel, such that hearts injected with highly spread hydrogels showed no conduction abnormalities. Conversely, the results of this study indicate that injection of a hydrogel exhibiting minimal interstitial spread may create a substrate for arrhythmia shortly after injection by causing LV activation delays and reducing gap junction density at the site of injection. Thus, this work establishes site of delivery and interstitial spread characteristics as important factors in the future design and use of biomaterial therapies for MI treatment.

Graphical Abstract

[*]Co-corresponding authors: Phone: (858) 822-6036; (858) 822-7863, Fax: (858) 534-5722, christman@bioeng.ucsd.edu.

Disclosures: Dr. Christman is co-founder, board member, and holds equity interest in Ventrix, Inc.

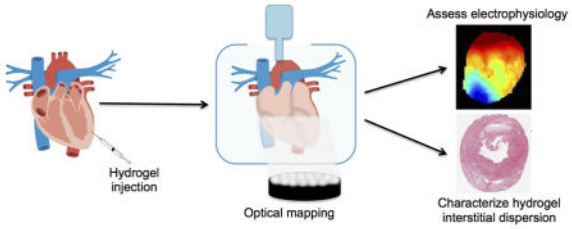

Keywords

biomaterial; myocardial infarction; optical mapping; electrophysiology

1. Introduction

With myocardial infarction (MI) affecting over one million Americans each year [1], there has been a push for the development of novel therapies for the treatment of MI, subsequent left ventricular (LV) remodeling and eventual heart failure (HF). The field of biomaterials for treating MI has rapidly expanded over the past decade and in particular, injectable biomaterials, including hydrogels, have been evaluated as potential minimally invasive therapies for MI and HF [2–4]. Injection of hydrogels composed of collagen [5, 6], alginate [7, 8], fibrin [9], chitosan [10], small intestinal submucosa [11], myocardial matrix [12, 13] and degradable synthetic materials [14–16] have shown therapeutic benefit in terms of global cardiac parameters such as improved or maintained left ventricular geometry and ejection fraction (EF). As these therapies show positive results with potential for catheter delivery in some cases [8, 12], injectable hydrogels are beginning to advance to large animal pre-clinical models [8, 13] and recently clinical trials [17, 18]. Several hydrogels have also shown success in improving cell transplant survival in the heart in animal models [2, 3, 19, 20]. With the promise of injectable hydrogels, it is exceedingly important to understand the mechanisms by which this type of biomaterial affects the underlying tissue and the impact on not only treatment of the pathological condition, but also patient safety.

Many patients eligible for a cell and/or biomaterial therapy may already be at increased risk of ventricular arrhythmia [21], so it is essential that the therapy does not increase the ventricular vulnerability above the baseline level. However, previous studies have shown that injection of certain cell types disturbs normal electrical propagation through the tissue and increases vulnerability to dangerous ventricular arrhythmias [22–24]. Along similar lines, injection of a hydrogel in the myocardium could cause conduction abnormalities and alter action potential propagation. If such changes occurred, the hydrogel could create a substrate for arrhythmia and ultimately a pose hazard to patient safety. However to date, studies aimed at understanding the effect of hydrogel injection on cardiac electrophysiology and arrhythmogenesis are lacking.

A variety of both biologically derived and synthetic hydrogels have been injected into infarcted tissue as a potential therapy for MI. There is heterogeneity in both the site of delivery and interstitial spread of these biomaterials. Injection of a hydrogel in the infarcted region of the myocardium has been advantageous through augmentation of LV wall

mechanics [5] and promoting cellular migration into the region [25]. In contrast, injection into the viable border zone has shown improved myocardial salvage and prevention of infarct expansion [26]. The latter is also a common injection site when delivering cells [27]. One concern is that the presence of the hydrogel in viable tissue may make that region vulnerable to alterations in electrical propagation. Another important concern is that different hydrogels demonstrate varying degrees of interstitial spread [28–30]. Hydrogels with low spread stay confined in a localized region resulting in myocardium being pushed to the perimeter of the hydrogel structure. In contrast, highly spread hydrogels occupy the interstitial space between neighboring cardiomyocytes resulting in the presence of myocardial fibers throughout the hydrogel structure. The amount of integration with the native myocardium may therefore influence how the hydrogel impacts the electrophysiological properties of the underlying tissue.

Optical mapping is widely established as a robust technique for the detection, visualization and quantification of electrophysiological changes in cardiac tissue [31]. This technology has been recently utilized for the assessment of changes in electrophysiology and potential arrhythmogenesis after infarction [32, 33] and cellular transplantation at the site of infarction [34, 35]. Herein, we utilize optical mapping as a tool to assess the effects of injection of a hydrogel with varying interstitial spread on LV activation and repolarization in healthy and cryoinfarcted hearts acutely following injection. This work assesses the potential of this type of biomaterial to become a substrate for arrhythmias.

2. Materials and Methods

All experiments in this study were conducted in accordance with the guidelines established by the Institutional Animal Care and Use Committee and the American Association for Accreditation of Laboratory Animal Care and were approved by the Institutional Animal Care and Use Committee at the University of California, San Diego.

2.1. Preparation of injectable materials

Hydrogels were prepared by mixing solutions of 4-arm polyethylene glycol-succinimidyl glutaramide (PEG-SGA, JenKem Technology USA, Plano, TX; 50 mg/mL in phosphate buffer pH 4.0) and 4-arm polyethylene glycol-amine (PEG-NH_2, JenKem Technology USA, Plano, TX; 50 mg/mL in borate buffer pH 8.0) to create PEG hydrogels by chemical crosslinking. PEG-ASG and PEG-NH_2 were combined in a 1:1 ratio and gelation occurred 40 seconds after mixing *in vitro*.

2.2. Experimental Design

Sixty-six Sprague-Dawley rats were divided into healthy (n = 31) and cryoinfarct (n = 35) groups. Healthy animals received either hydrogel injection (n = 15), saline injection (n = 8) or no injection (n = 8) into the LV free wall. Animals undergoing the cryoinfarct surgery were allowed to recover for one-week prior to injection surgeries. At the time of injection surgery animals were divided into treatment groups: hydrogel injection into the borderzone (n = 17) or no injection (n = 18). Twenty-minutes after injection, the hearts were excised and hung on a Langendorff apparatus to complete optical mapping experiments. After

completing the mapping, hearts were prepared for histological analysis. Specific methods are detailed below.

2.3. Cryoinfarction surgery

Female Sprague Dawley rats were anesthetized using 5% isoflurane, intubated and maintained at 2.5% isoflurane for the surgery procedure. A left thoracotomy was used to access the heart. A custom cryoprobe filled with liquid nitrogen was held at the apical end of the LV free wall for thirty seconds to create the cryoinfarct. The animals were sutured closed and allowed to recover. One week after cryoinfarction, hemodynamic measurements and an injection surgery were performed as described below for hydrogel-injected and non-injected groups. Hydrogel injections were made at the border zone of the basal side of the infarct. Cryoinfarct location was selected so that the entire injury would be visible in the imaging frame and so that hydrogel injections could be made in a similar location to healthy hearts. If the probe location was inconsistent leading to a cryoinfarct that was too close to the apex (out of the viewing frame) or too close to the base (interfering with hydrogel injection) the hearts were excluded from analysis (n = 4 excluded from each group). No mortality occurred during these procedures.

2.4 In vivo hemodynamic measurements and injection surgery

Female Sprague Dawley rats were anesthetized using 5% isoflurane, intubated and maintained at 2.5% isoflurane for the surgery procedure. The animals were ventilated using a respirator at 75 breaths/minute. The right carotid artery was carefully isolated and a pressure transducer (Millar; SPR-407) was inserted in through the carotid artery and advanced into the left ventricle. The isoflurane was reduced to 1% and the ECG and LV pressures were monitored and recorded. End diastolic pressure (EDP) was defined as the LV pressure at the peak of the QRS complex while peak systolic pressure (PSP) was established as the maximum LV pressure. All pressure measurements were averaged over 10 beats in the cardiac cycle. After acquiring pressure measurements, the heart was exposed using a left anterior thoracotomy and injected once with either 75 μl of the hydrogel or saline using a 27 G needle into LV free wall or not injected as a sham group. To create a range of resulting interstitial spread of the hydrogel, the mixed solution was injected into the LV myocardium between 25 and 35 seconds after mixing. In general, the earlier the mixture was injected, the more interstitial spread occurred before gelation and vice versa. There was some variability in spread within one injection time point, but this method enabled a broader range of interstitial spread from approximately 20 to 50 % (Figure S1). Isoflurane was maintained at 2.5% during the injection procedure. Presence of the injection was verified by temporary discoloration of the tissue. If the hydrogel was partially or fully extruded from the tissue immediately following injection the hearts were excluded from the study (n = 3 healthy and n = 3 cryoinfarcted excluded). Post-injection hemodynamic parameters were measured 20 minutes after injection, or an equivalent time point after the heart was exposed for non-injected controls, as described at baseline. No mortality occurred during these procedures.

2.5. Optical mapping of the polymer injection in Langendorff-perfused rat heart

Final group numbers that were included in the optical mapping analysis were as follows: healthy (hydrogel: n = 12, saline: n = 8, no injection: n = 8) and cryoinjured (hydrogel: n =

10, no injection: n = 14. Immediately after post-injection hemodynamic measurements (20 minutes post-injection), the hearts were excised and arrested using a solution containing 25 mM $NaHCO_3$, 2 mM $CaCl_2$, 5 mM Dextrose, 2.7 mM $MgSO_4$, 22.8 mM KCl, 121.7 mM NaCl, 20 mM 2,3 butanedione monoxime. The aorta of the heart was cannulated and attached to a Langendorff apparatus. The hearts were then retrograde perfused with a Tyrode's solution (25 mM $NaHCO_3$, 2 mM $CaCl_2$, 5 mM Dextrose, 2.7 mM $MgSO_4$, 4.8 mM KCl, 121.7 mM NaCl, 10 mM Blebbistatin) at 37° C in a custom designed optical mapping chamber. A constant pressure of 70 mmHg was maintained and the flow rate was monitored. Blebbistatin (EMD Millipore, Darmstadt, Germany) was used as an electromechanical decoupler as previously shown to minimize motion artifact [36].

The heart was stained with the voltage sensitive fluorescent dye di-4-ANEPPS (Biotium, Hayward, CA) that was dissolved in dimethysulfoxide (DMSO) and diluted to 5.2 mM with Tyrode's solution. A 10 mL bolus of this solution was injected into the perfusion line. The LV free wall was imaged with a high-speed CMOS camera (MiCAM Ultima L, Brainvision) using a custom-built tandem lens imaging system, with an objective lens of 0.5X and imaging lens of 1X (Leica planapo objective). Images were collected with a spatial and temporal resolution of 100 × 100 pixels at 0.2 mm × 0.2 mm per pixel, and a frame rate of 1000 frames per second. The dye-stained LV epicardial surface was excited by an LED lamp (LEDtronics) at 470 nm (excitation of the LED lamps) and the emitted fluorescence was collected and filtered with a long-pass filter >610 nm (Figure 1). The images were collected at intrinsic cardiac rhythm.

2.6. Data analysis

Optical signals were imported into Matlab and analyzed using custom software as previously described [37]. Briefly, activation time was identified at each pixel as the time of maximum rate of change of fluorescence for the action potential upstroke for each beat $(dF/dt)_{max}$. To calculate the time of repolarization, the time at which the action potential recovered to 20%, 50%, and 80% of the peak value were determined. The action potential duration (APD) at 20%, 50%, and 80% were calculated as the difference between repolarization time at the respective level and activation time of the action potential. The dispersion in APD and repolarization times was calculated as the difference between the maximum and minimum APD or repolarization time over the LV epicardium in the field of view respectively. Heterogeneities in dye perfusion created increasing variability in dispersion values at longer repolarization times. Therefore dispersion in APD and repolarization in healthy hearts were only determined at 20% repolarization. Furthermore due to the resultant dye perfusion differences in the cryoinfarcted hearts (ie. non-perfused infarcts), dispersion values were not determined in these hearts.

2.7. Histology

After the completion of the optical mapping experiments, the heart was removed from the cannula, embedded and fresh frozen in Tissue-Tek O.C.T. freezing compound. Short axis cross sections (10 μm thick) were taken every 350 μm from apex to base and stained with hematoxylin and eosin (H&E). Cryoinjury size, measured as percent of LV circumferences, was quantified as previously described [38]. Slides were imaged with a Carl Zeiss Observer

D.1 and hydrogel spread was quantified using Photoshop software (Adobe Photoshop CS3). Specifically, the injection region was selected to include the hydrogel with any respective penetrating muscle. The hydrogel within the injection region was identified by the lightly pink stained material, and histological artifacts were carefully avoided in all measurements. The pixel count was recorded for both the 'injection' and 'hydrogel' regions for each heart slice. Known spacing between slices enabled calculation of 'injection volume' and 'hydrogel volume' and the percent muscle within the hydrogel was determined as:

$$Percent\ muscle\ within\ hydrogel = \left[\frac{Volume_{Injection} - Volume_{hydrogel}}{Volume_{Injection}}\right] \times 100$$

2.8. Gap junction staining and quantification

To assess gap junction density, immunohistochemistry was performed on two representative slides from each heart. Slides containing the largest area of hydrogel were used in the hydrogel group, and equivalent anatomical locations were used in non-injected and saline-injected hearts. Cryosections were fixed with acetone, incubated with anti-connexin 43 antibody (EMD Millipore, Billerica, MA; 1:200 dilution) and anti-cardiac troponin antibody (Abcam, Cambridge, United Kingdom; 1:100 dilution), and then stained with Alexa Fluor 568 anti-mouse antibody (Invitrogen, Carlsbad, CA; 1:500 dilution) and Alexa Fluor 488 anti-rabbit antibody (Invitrogen, Carlsbad, CA; 1:500 dilution). Nuclei were visualized with fluorescent Hoechst 33342. Slides were imaged using a Leica DM6000B (Leica Microsystems Inc, Buffalo Grove, IL) immune-fluorescent microscope at 20x magnification and analyzed using a proprietary Leica software suite. Gap junction densities in the hydrogel groups were measured in the injection regions as well as in a region on the LV free wall adjacent to the injection. A representative area within the LV free wall was selected for analysis in all other groups. Gap junction density was calculated as:

$$Gap\ junction\ density = \left[\frac{Area\ of\ connexin43\ positive\ staining}{\#\ of\ nuclei}\right]$$

2.9. Statistical analysis

A one-way analysis of variance (ANOVA) test with a Dunnet post-hoc test analysis was used to detect differences among groups for the pressure measurements. ANOVA with Newman-Keuls post-hoc analysis was used to detect differences in LV activation time in healthy hearts, in dispersion of APD and repolarization at 20%, as well as in gap junction densities between groups. A t-test was used to compare LV activation times of cryoinfarcted heart treatment groups. Correlation analysis was performed to determine whether LV activation time, dispersion of 20% repolarization and gap junction density depended on the percent muscle within the hydrogel injection. All measurements were reported mean ± SEM, unless otherwise specified. Significance was accepted at $p < 0.05$.

3. Results

3.1. Hemodynamic measurements

Hemodynamic measurements were performed at baseline to ensure normal cardiac behavior prior to the injection surgery and also as a comparison between injected and non-injected hearts prior to optical mapping. The average baseline LV EDP and PSP in the rat hearts included in the study was 8.31 ± 1.02 mmHg and 96.02 ± 11.8 mmHg respectively, signifying normal cardiac function. Measurement of the hemodynamic properties acutely after injection demonstrated no statistical differences in LV EDP and PSP between injected hearts and respective non-injected controls, indicating no acute changes in hemodynamic parameters upon injection of the biomaterials (Table 1).

3.2. Optical mapping and histological analysis

Immediately after post-injection hemodynamic measurements the hearts were excised and arrested. Electrical propagation in the isolated rat heart was studied using a Langendorff, aorta-perfused setup. Fluorescent images of the epicardial surface of the hearts were obtained to verify the perfusion of the dye over the entire healthy epicardium; the dye did not perfuse the cryoinfarct region (Figure 2A & 2E, respectively). Histological analysis was performed upon completion of the optical mapping study to verify the presence and distribution of material in the injection region. In Figure 2B & 2F the hydrogel injection region is clearly visible as denoted by the black arrows. Non-injected and saline-injected healthy heart slices are shown for comparison (Figure 2C & 2D, respectively). In Figure 2F and 2G the cryoinfarct is visible and denoted by red arrows for hydrogel-injected and non-injected hearts, respectively.

3.3. Action potential propagation

The timing of hydrogel injection was varied to generate a wide range of interstitial spread (Figure S1; $r = -0.48$; $p < 0.03$). For initial analysis all hydrogel-injected hearts were combined into one group. To detect any alterations in action potential propagation due to the presence of the hydrogel, LV activation maps were constructed to depict action potential propagation. Representative color maps indicate that LV activation times were higher in the healthy hydrogel-injected hearts compared to non-injected and saline-injected, particularly towards the base (Figure 3A). When including all degrees of hydrogel spread, on average injection of the hydrogel led to a significant increase in total LV activation time, 5.2 ± 0.4 ms compared to saline 3.5 ± 0.4 ms ($p < 0.01$) and no-injection 4.1 ± 0.2 ms ($p < 0.05$), indicating slowed action potential propagation across the LV (Figure 3B). To determine whether similar increases in LV activation time would occur following hydrogel injection in infarcted hearts, the hydrogel was injected into the borderzone one week following cryoinfarction surgery. There was no difference in cryoinfarct size between hydrogel-injected (22 ± 3%) and non-injected controls (18 ± 2%). Again significantly higher LV activation times were observed following hydrogel injection, 6.1 ± 0.4, compared to no-injection, 4.6 ± 0.3 ($p < 0.02$; Figure 3C & 3D), revealing slowed action potential propagation through hydrogel-injected tissue bordering an infarct.

To investigate the effect of hydrogel spread on action potential propagation, the amount of myocardium penetrating the hydrogel in each heart was determined histologically. High and low percent muscle within the hydrogel was the metric used to define high and low interstitial spread, respectively. Representative images of hydrogels exhibiting low and high interstitial spread are shown in Figure 4A–D. The percent muscle within the hydrogel was then compared to the LV activation time for each heart. There was a significant correlation between the percent of muscle within the hydrogel injection and the LV activation time for healthy ($r = -0.78$; $p < 0.01$; Figure 4E) and cryoinfarcted ($r = -0.93$; $p < 0.0001$; Figure 4F) hearts. Specifically, lower LV activation times, comparable to non-injected hearts, occurred in hearts with high percent muscle within the hydrogel (>35%), whereas when the percent muscle in the hydrogel was low (<35%), the LV activation times were higher, indicative of slowed conduction. The combined distribution for all hydrogel injected hearts is shown in Figure 4G ($r = -0.85$; $p < 0.0001$). We compared the hydrogel volume in each heart to the percent muscle within the hydrogel (Figure S2A) as well as to the activation time (Figure S2B) and found no correlation ($r = -0.31$; $p = 0.18$ and $r = 0.17$; $p = 0.48$, respectively). Thus, injection of highly spread hydrogels caused no change in action potential propagation across the LV, but propagation was slowed following injection of minimally spread hydrogels.

3.4. Changes in other electrophysiological parameters

Dispersion in action potential duration (APD) and repolarization can increase the likelihood for reentrant arrhythmias by creating local disturbances in the tissue [39]. Measurements of action potential characteristics such as APD at 20%, 50% and 80% repolarization levels demonstrate no significant changes in APD_{20}, APD_{50} and APD_{80} by the injection of the hydrogel in healthy or cryoinfarcted hearts (Table 2). There were similarly no differences in dispersion of APD_{20} between groups in healthy hearts (Figure 5A). However, there was a trend for increased dispersion at 20% repolarization in the hydrogel-injected healthy hearts compared to the saline and no injection groups ($p = 0.06$; Figure 5B). Color maps were created to visualize the time of 20% repolarization at each pixel on the epicardium, which revealed increase 20% repolarization times at the base of some hydrogel-injected healthy hearts (Figure 5C). Furthermore, a higher percent of muscle within the hydrogel injection significantly correlated with a lower dispersion of 20% repolarization ($r = -.0.67$; $p < 0.03$). This indicates that the degree of interstitial spread of the hydrogel also impacted the dispersion of repolarization in healthy hearts. As described in the methods section, the absence of dye perfusion in the cryoinfarct resulted in increased variability in repolarization times and thus these values were not reported. Specifically, a highly spread hydrogel did not create heterogeneities in action potential characteristics, while such variability was observed following injection of a hydrogel with low spread.

3.5. Impact of polymer interstitial spread on gap junction density

To better understand the mechanism behind the effect of hydrogel interstitial spread on action potential propagation, the gap junction densities (Cx43+ area per nuclei) within the hydrogel injection and a region adjacent to the hydrogel were quantified. For comparison, gap junction density within a representative area of the LV free wall was quantified for non-injected and saline-injected groups. Again including all degrees of hydrogel spread, when

compared to all other groups, gap junction densities within the hydrogel injection site were significantly lower on average for both healthy (Figure 6A; $p < 0.0005$) and cryoinfarcted (Figure 6B; $p < 0.0001$) hearts. Comparison of hydrogel spread and gap junction density revealed that an increase in the percent muscle within the hydrogel injection in healthy and cryoinfarcted hearts correlated with an increase in gap junction density ($r = 0.66$; $p < 0.005$; Figure 6C). Gap junction densities within the highly spread hydrogels were close to the densities observed in non-injected hearts, yet were lower within the less spread hydrogels. A representative image of the 'normal' gap junction density of non-injected/saline-injected hearts is shown in Figure 6D along with the densities in the injection site of a hydrogel with high and low interstitial spread (Figures 6E and 6F, respectively).

4. Discussion

With the rapid increase in potential injectable biomaterial therapies for myocardial repair after infarction, the question of safety of biomaterial injection is an important issue and pre-requisite to clinical translation. In this study the important, but often overlooked issue of electrophysiological impact of hydrogel injection during these procedures was studied. Utilizing optical mapping, we were able to assess the acute effect of intramyocardial injection of a hydrogel on the global electrophysiological parameters – activation time, APD, and repolarization. Most importantly, we found that injection of a hydrogel with high interstitial spread did not affect LV activation time, while injection of a hydrogel with low interstitial spread significantly increased this parameter. Using the metric of 'percent muscle within the hydrogel' to quantify hydrogel spread, we found that a hydrogel injection containing >35% muscle did not increase the LV activation time compared to non-injected hearts (Figure 4). Similarly, these highly spread hydrogels did not increase dispersion of repolarization (Figure 5D). Interestingly, we did not observe any differences in APD between hydrogel-injected and non-injected hearts. Thus the electrophysiological impact of the minimally spread hydrogel injection was through delaying action potential propagation across the LV, rather than altering the action potential morphology.

A potential mechanism by which the injection of the hydrogels with low interstitial spread caused slowed action potential propagation may be the disruption of gap junctions between the conductive cardiomyocytes. Disturbance in gap junctions has been associated with induction of harmful ventricular arrhythmias in small animal studies [40]. Here we show that cardiac muscle within the hydrogels with low spread had a reduced gap junction density compared to muscle penetrating highly spread hydrogels. There was likely a combination of factors that lead to the rapid reduction of gap junction density following hydrogel injection. First, connexin43 is rapidly turned over in healthy rat hearts, with a half-life of just over one hour [41]. Furthermore, one response of cardiomyocytes under lethal and sub-lethal stress is a reduction in gap junction density [41]. Thus under the stress of muscle fibers being physically separated by the hydrogel, the cardiomyocytes in the injection region may have initiated a survival response that included reducing gap junction density. In combination with the already rapid connexin43 turnover rate this could result in low gap junction densities just twenty minutes after hydrogel injection. Gap junction density in the myocardium adjacent to the injection region was unaffected.

The clinically relevant question is whether or not slowing of action potential propagation and reduced gap junction density caused by injection of a hydrogel with low interstitial spread would lead to ventricular arrhythmias. Van Rijen et al. showed that through conditional deletion of connexin43 (Cx43) in adult mice, >70% reduction in Cx43 protein expression was required to significantly slow conduction velocity (CV) and enhance arrhythmogenesis [42]. Even with a 50% reduction in Cx43 expression, CV was maintained at normal levels. In our study, when the hydrogel spread was low enough to cause high LV activation time (<35% muscle in the injection, Figure 4), gap junction densities inside the hydrogel were on average >70% reduced compared to healthy myocardium (Figure 6). This suggests that the disruption may be enough to enhance arrhythmogenesis. In contrast, in hearts injected with highly spread hydrogels that did not increase global activation time (>35% muscle in the injection, Figure 4), gap junction densities within the injection tended to be <70% reduced (Figure 6), reducing the risk for arrhythmogenesis based solely on gap junction density.

The gap junction density and distribution seen in the less spread hydrogels (Figure 6E) also looked remarkably similar to that observed by Van Veen et al. in mice with severe interstitial fibrosis caused by aging and a 50% knockdown of the Scn5a sodium channel [43]. Fibrosis has been indicated as a substrate for reentrant arrhythmia in patients with dilated cardiomyopathy [44]. This and other studies [45] have indicated the architecture of the fibrosis as a factor in whether or not conduction block was observed. Small amounts of interstitial fibrosis did not appear to disrupt lateral cell-cell connections, mitigating the generation of anisotropic conduction [44, 45]. Thus, based on comparable disruption of cell-cell coupling, the hydrogel with low spread may act as a substrate for arrhythmia in a similar manner to severe fibrosis. Furthermore, it is also possible that the degree of interstitial spread impacted the stiffness of the hydrogel, which may have contributed in part to the observed differences in conduction. Finally, it is now widely accepted that cardiac electrical conduction is a function of not only the cellular conductivity but also the conductivity of the extracellular space [46, 47]. The presence of a hydrogel with different electrical properties than the native extracellular matrix could affect the local extracellular conductivity, though this warrants further study. All these studies suggest that distribution in the tissue is an important factor to consider when designing injectable biomaterial therapies for MI.

Controlling how much hydrogels spread in the tissue is complex due to contribution of several factors. For example, gelation mechanism, injection time and material concentration could all be modified to achieve varying interstitial spread. In this study, we varied injection time of a model PEG hydrogel to allow for a wide range in the degree of hydrogel spread in the tissue. We chose a PEG hydrogel with a polymer content of 50 mg/mL to create a gel with mechanical properties within the range of other commonly injected material for biomaterial MI therapy [27, 48]. Selecting a concentration in the middle of the range allowed access to both high and low amounts of interstitial spread. Other material properties could however be modulated to achieve differences in interstitial spread. For example, materials such as alginate can be crosslinked *in situ* following intracoronary infusion, which leads to greater interstitial spread of the material in the tissue. In fact both large animal studies [8] and initial clinical trials [17, 18] show no evidence of arrhythmias with this

material. Moreover, other materials with higher interstitial spread such as a myocardial matrix hydrogel have not been shown to elicit arrhythmias in large animal models [13]. In contrast, other studies using materials, which appear to have lower interstitial spread, have had potential indicators of arrhythmias. Injection of a different alginate formulation into a chronic canine heart failure model (microembolization) was non-arrhythmogenic in the long-term; however, one hydrogel-injected dog died from ventricular fibrillation shortly after the injection [49]. The histological images of the injected dog hearts reveal fairly low interstitial spread [49], which may have contributed to the rhythm disturbance in the animal that died post-injection. Another fast gelling hydrogel system, a fibrin-alginate composite, was injected into infarcted porcine myocardium [50]; the authors noted that mortality was higher in hydrogel-injected animals, which they believed warrants further study into the impact of the hydrogel on electrical activation patterns. While the exact cause in both studies cannot be definitively determined given even needle penetration into the myocardium can cause ventricular arrhythmias, these studies along with the results of the current study, suggest that the link between material properties and arrhythmia vulnerability should be continued to be carefully studied prior to clinical translation. This study only investigated the impact of hydrogels, but micro- and nano-particles are another commonly used form of biomaterial for treating cardiovascular disease [51]. These particles typically spread well through the interstitial space and consequently should, based on the results of the current study, provide minimal disruption to cardiac conduction.

Previous studies have shown that the infarct already has slowed or disturbed conduction [32], so injection of a hydrogel into the infarct may not cause conduction abnormalities superseding the effects of infarction injury. In a study by Singelyn et al., arrhythmogenesis was assessed in rat MI model one week after injection of a myocardial matrix hydrogel in the infarct region and there were no increases in incidences of arrhythmia [12]. Similar results were seen after both intracoronary and intramyocardial injection of different hydrogels in a porcine infarct [8, 20]. On the other hand, the borderzone contains electrically viable and vulnerable tissue, so injection or spread of material into this region could be a concern. Herein, we injected a hydrogel first in viable myocardium to specifically understand the acute effect of material injection and interstitial spread on myocardial tissue containing viable myocytes. Subsequently we injected the hydrogel into the borderzone of an infarct to determine if viable myocardium bordering the injury was susceptible to the same alterations in action potential propagation. One limitation of this study is the use of a rodent model instead of a large animal model; this was chosen given the high number of animals needed to complete a thorough investigation of hydrogel spread on conduction. In addition, it is acknowledged that the cryoinjury model is not as physiologically relevant as an occlusion model, but it was selected because it allowed dye perfusion of the viable myocardium. Since the dye is introduced to the tissue through retrograde perfusion total occlusion and ischemia-reperfusion models of MI create permanent damage to the vessels preventing sufficient dye perfusion for imaging. The cryoinjury model also enabled control over the location of the infarct and was initiated on the epicardial surface, facilitating consistency across the hearts and clear visualization with the *ex vivo* imaging. In both healthy and cryoinfarcted rat hearts, injection of a highly spread hydrogel into viable myocardium resulted in no change to the LV activation time compared to non-injected

controls, while hydrogel injections with low spread increased LV activation time shortly after injection.

In this acute study, PEG was selected due to its bio-inert characteristics in order to isolate and model the impact of the physical presence of a hydrogel on heart electrophysiology. The hydrogel-injected hearts were excised within one hour of injection because a major concern with arrhythmias is in the acute phase following injection. Our study suggests that it is ultimately important how the injected material resides within the myocardium. Thus, negative initial impacts on electrophysiology can be potentially avoided by designing the material to spread well within the myocardium, and/or injecting into solely the infarct instead of the borderzone. Given the difference in the size and heart rate of the human heart compared to a rodent heart, it will, however, be important to study these parameters in large animal models. Moreover, at later time points, degradation of the biomaterial and resulting cell infiltration will both contribute to its level of risk of becoming a substrate for arrhythmia, and therefore, it is also important to continue to study the risk of arrhythmias for each individual biomaterial over time prior to use in patients.

5. Conclusions

Injection of a highly spread hydrogel in the myocardium does not alter action potential propagation soon after injection, while injection of a hydrogel with low spread may create a substrate for arrhythmia by causing slowed action potential propagation through reduced gap junction density at the site of injection. While injection into the infarct may not be a concern given the already slowed or perturbed conduction, our results indicate that delivery of a highly spread hydrogel into viable or border zone myocardium is safe whereas a hydrogel with low spread may have deleterious acute effects. This work establishes site of delivery and spread of biomaterials in the tissue as important factors in the future use and development of biomaterial therapies for MI treatment, and warrants further investigation in large animal models.

Supplementary Material

Refer to Web version on PubMed Central for supplementary material.

Acknowledgments

Funding Sources: This research was supported in part by National Institutes of Health (NIH) through R01HL113468 and through the NIH Director's Transformative Research Award (5R01HL117326), part of the NIH Common Fund. A.A.R and S.L.S. would like to thank the National Science Foundation for Graduate Research Fellowships.

References

1. Roger VL, Go AS, Lloyd-Jones DM, Benjamin EJ, Berry JD, Borden WB, et al. Heart disease and stroke statistics--2012 update: a report from the American Heart Association. Circulation. 2012; 125:e2–e220. [PubMed: 22179539]
2. Christman KL, Lee RJ. Biomaterials for the treatment of myocardial infarction. J Am Coll Cardiol. 2006; 48:907–13. [PubMed: 16949479]

3. Rane AA, Christman KL. Biomaterials for the Treatment of Myocardial Infarction. J Am Coll Cardiol. 2011; 58:2615–29. [PubMed: 22152947]
4. Johnson TD, Christman KL. Injectable hydrogel therapies and their delivery strategies for treating myocardial infarction. Expert Opinion on Drug Delivery. 2013; 10:59–72. [PubMed: 23140533]
5. Dai W, Wold LE, Dow JS, Kloner RA. Thickening of the infarcted wall by collagen injection improves left ventricular function in rats: a novel approach to preserve cardiac function after myocardial infarction. J Am Coll Cardiol. 2005; 46:714–9. [PubMed: 16098441]
6. Blackburn NJR, Sofrenovic T, Kuraitis D, Ahmadi A, Mcneill B, Deng C, et al. Timing underpins the benefits associated with injectable collagen biomaterial therapy for the treatment of myocardial infarction. Biomaterials. 2015; 39:182–92. [PubMed: 25468370]
7. Landa N, Miller L, Feinberg MS, Holbova R, Shachar M, Freeman I, et al. Effect of injectable alginate implant on cardiac remodeling and function after recent and old infarcts in rat. Circulation. 2008; 117:1388–96. [PubMed: 18316487]
8. Leor J, Tuvia S, Guetta V, Manczur F, Castel D, Willenz U, et al. Intracoronary injection of in situ forming alginate hydrogel reverses left ventricular remodeling after myocardial infarction in Swine. J Am Coll Cardiol. 2009; 54:1014–23. [PubMed: 19729119]
9. Christman KL, Fok HH, Sievers RE, Fang Q, Lee RJ. Fibrin glue alone and skeletal myoblasts in a fibrin scaffold preserve cardiac function after myocardial infarction. Tissue Eng. 2004; 10:403–9. [PubMed: 15165457]
10. Lu WN, Lü SH, Wang HB, Li DX, Duan CM, Liu ZQ, et al. Functional improvement of infarcted heart by co-injection of embryonic stem cells with temperature-responsive chitosan hydrogel. Tissue Eng Pt A. 2009; 15:1437–47.
11. Okada M, Payne TR, Oshima H, Momoi N, Tobita K, Huard J. Differential efficacy of gels derived from small intestinal submucosa as an injectable biomaterial for myocardial infarct repair. Biomaterials. 2010; 53:7678–83. [PubMed: 20674011]
12. Singelyn JM, Sundaramurthy P, Johnson TD, Schup-Magoffin PJ, Hu DP, Faulk DM, et al. Catheter-deliverable hydrogel derived from decellularized ventricular extracellular matrix increases endogenous cardiomyocytes and preserves cardiac function post-myocardial infarction. J Am Coll Cardiol. 2012; 59:751–63. [PubMed: 22340268]
13. Seif-Naraghi SB, Singelyn JM, Salvatore MA, Osborn KG, Wang JJ, Sampat U, et al. Safety and Efficacy of an Injectable Extracellular Matrix Hydrogel for Treating Myocardial Infarction. Science Translational Medicine. 2013; 5:173ra25–ra25.
14. Jiang XJ, Wang T, Li XY, Wu DQ, Zheng ZB, Zhang JF, et al. Injection of a novel synthetic hydrogel preserves left ventricle function after myocardial infarction. Journal of biomedical materials research Part A. 2009; 90:472–7. [PubMed: 18546187]
15. Fujimoto KL, Ma Z, Nelson DM, Hashizume R, Guan J, Tobita K, et al. Synthesis, characterization and therapeutic efficacy of a biodegradable, thermoresponsive hydrogel designed for application in chronic infarcted myocardium. Biomaterials. 2009; 30:4357–68. [PubMed: 19487021]
16. Wang T, Wu DQ, Jiang XJ, Zhang XZ, Li XY, Zhang JF, et al. Novel thermosensitive hydrogel injection inhibits post-infarct ventricle remodelling. Eur J Heart Fail. 2009; 11:14–9. [PubMed: 19147452]
17. Frey N, Linke A, Suselbeck T, Muller-Ehmsen J, Vermeersch P, Schoors D, et al. Intracoronary Delivery of Injectable Bioabsorbable Scaffold (IK-5001) to Treat Left Ventricular Remodeling After ST-Elevation Myocardial Infarction: A First-in-Man Study. Circulation: Cardiovascular Interventions. 2014; 7:806–12. [PubMed: 25351198]
18. Bellerophon BCM LLC. [Accessed 6 March 2015] NCT01226563: IK-5001 for the Prevention of Remodeling of the Ventricle and Congestive Heart Failure After Acute Myocardial Infarction (PRESERVATION 1). 2015. Available at https://clinicaltrials.gov/ct2/show/NCT01226563
19. Guo H-D, Wang H-J, Tan Y-Z, Wu J-H. Transplantation of Marrow-Derived Cardiac Stem Cells Carried in Fibrin Improves Cardiac Function After Myocardial Infarction. Tissue Engineering Part A. 2011; 17:45–58. [PubMed: 20673001]

20. Lin Y-D, Yeh M-L, Yang Y-J, Tsai D-C, Chu T-Y, Shih Y-Y, et al. Intramyocardial Peptide Nanofiber Injection Improves Postinfarction Ventricular Remodeling and Efficacy of Bone Marrow Cell Therapy in Pigs. Circulation. 2010; 122:S132–S41. [PubMed: 20837904]
21. Menasche P. Stem Cell Therapy for Heart Failure: Are Arrhythmias a Real Safety Concern? Circulation. 2009; 119:2735–40. [PubMed: 19470902]
22. Hagège AA, Marolleau JP, Vilquin JT, Alhéritière A, Peyrard S, Duboc D, et al. Skeletal myoblast transplantation in ischemic heart failure: long-term follow-up of the first phase I cohort of patients. Circulation. 2006; 114:I108–13. [PubMed: 16820558]
23. Dib N, Michler RE, Pagani FD, Wright S, Kereiakes DJ, Lengerich R, et al. Safety and feasibility of autologous myoblast transplantation in patients with ischemic cardiomyopathy: four-year follow-up. Circulation. 2005; 112:1748–55. [PubMed: 16172284]
24. Siminiak T, Kalawski R, Fiszer D, Jerzykowska O, Rzeźniczak J, Rozwadowska N, et al. Autologous skeletal myoblast transplantation for the treatment of postinfarction myocardial injury: phase I clinical study with 12 months of follow-up. Am Heart J. 2004; 148:531–7. [PubMed: 15389244]
25. Huang NF, Yu J, Sievers R, Li S, Lee RJ. Injectable biopolymers enhance angiogenesis after myocardial infarction. Tissue Eng. 2005; 11:1860–6. [PubMed: 16411832]
26. Hsieh PCH. Controlled delivery of PDGF-BB for myocardial protection using injectable self-assembling peptide nanofibers. Journal of Clinical Investigation. 2005; 116:237–48. [PubMed: 16357943]
27. Lu WN, Lu SH, Wang HB, Li DX, Duan CM, Liu ZQ, et al. Functional improvement of infarcted heart by co-injection of embryonic stem cells with temperature-responsive chitosan hydrogel. Tissue Eng Part A. 2009; 15:1437–47. [PubMed: 19061432]
28. Ifkovits JL, Tous E, Minakawa M, Morita M, Robb JD, Koomalsingh KJ, et al. Injectable hydrogel properties influence infarct expansion and extent of postinfarction left ventricular remodeling in an ovine model. Proc Natl Acad Sci USA. 2010; 107:11507–12. [PubMed: 20534527]
29. Christman KL, Vardanian AJ, Fang Q, Sievers RE, Fok HH, Lee RJ. Injectable fibrin scaffold improves cell transplant survival, reduces infarct expansion, and induces neovasculature formation in ischemic myocardium. J Am Coll Cardiol. 2004; 44:654–60. [PubMed: 15358036]
30. Davis ME, Hsieh PCH, Takahashi T, Song Q, Zhang SG, Kamm RD, et al. Local myocardial insulin-like growth factor 1 (IGF-1) delivery with biotinylated peptide nanofibers improves cell therapy for myocardial infarction. Proc Natl Acad Sci USA. 2006; 103:8155–60. [PubMed: 16698918]
31. Efimov IR, Nikolski VP, Salama G. Optical imaging of the heart. Circulation Research. 2004; 95:21–33. [PubMed: 15242982]
32. Mills WR, Mal N, Forudi F, Popovic ZB, Penn MS, Laurita KR. Optical mapping of late myocardial infarction in rats. Am J Physiol Heart Circ Physiol. 2006; 290:H1298–306. [PubMed: 16214848]
33. Ding C, Gepstein L, Nguyen DT, Wilson E, Hulley G, Beaser A, et al. High-resolution optical mapping of ventricular tachycardia in rats with chronic myocardial infarction. Pacing Clin Electrophysiol. 2010; 33:687–95. [PubMed: 20180914]
34. Gepstein L, Ding C, Rehemedula D, Wilson EE, Yankelson L, Caspi O, et al. In vivo assessment of the electrophysiological integration and arrhythmogenic risk of myocardial cell transplantation strategies. Stem Cells. 2010; 28:2151–61. [PubMed: 20960511]
35. Costa AR, Panda NC, Yong S, Mayorga ME, Pawlowski GP, Fan K, et al. Optical mapping of cryoinjured rat myocardium grafted with mesenchymal stem cells. Am J Physiol Heart Circ Physiol. 2012; 302:H270–7. [PubMed: 22037193]
36. Fedorov VV, Lozinsky IT, Sosunov EA, Anyukhovsky EP, Rosen MR, Balke CW, et al. Application of blebbistatin as an excitation-contraction uncoupler for electrophysiologic study of rat and rabbit hearts. Heart Rhythm. 2007; 4:619–26. [PubMed: 17467631]
37. Sung D, JSJPC, Mills R, McCulloch AD. Phase shifting prior to spatial filtering enhances optical recordings of cardiac action potential propagation. Ann Biomed Eng. 2001; 29:854–61. [PubMed: 11764316]

38. Robey TE, Murry CE. Absence of regeneration in the MRL/MpJ mouse heart following infarction or cryoinjury. Cardiovasc Pathol. 2008; 17:6–13. [PubMed: 18160055]
39. Sampson KJ, Henriquez CS. Electrotonic influences on action potential duration dispersion in small hearts: a simulation study. Am J Physiol Heart Circ Physiol. 2005; 289:H350–60. [PubMed: 15734889]
40. Danik SB, Liu F, Zhang J, Suk HJ, Morley GE, Fishman GI, et al. Modulation of cardiac gap junction expression and arrhythmic susceptibility. Circulation Research. 2004; 95:1035–41. [PubMed: 15499029]
41. Saffitz JE, Schuessler RB, Yamada KA. Mechanisms of remodeling of gap junction distributions and the development of anatomic substrates of arrhythmias. Cardiovascular Research. 1999; 42:309–17. [PubMed: 10533569]
42. Van Rijen HVM. Slow Conduction and Enhanced Anisotropy Increase the Propensity for Ventricular Tachyarrhythmias in Adult Mice With Induced Deletion of Connexin43. Circulation. 2004; 109:1048–55. [PubMed: 14967725]
43. Van Veen TAB. Impaired Impulse Propagation in Scn5a-Knockout Mice: Combined Contribution of Excitability, Connexin Expression, and Tissue Architecture in Relation to Aging. Circulation. 2005; 112:1927–35. [PubMed: 16172272]
44. Wu TJ, Ong JJ, Hwang C, Lee JJ, Fishbein MC, Czer L, et al. Characteristics of wave fronts during ventricular fibrillation in human hearts with dilated cardiomyopathy: role of increased fibrosis in the generation of reentry. Journal of the American College of Cardiology. 1998; 32:187–96. [PubMed: 9669269]
45. Kawara T, Derksen R, de Groot JR, Coronel R, Tasseron S, Linnenbank AC, et al. Activation delay after premature stimulation in chronically diseased human myocardium relates to the architecture of interstitial fibrosis. Circulation. 2001; 104:3069–75. [PubMed: 11748102]
46. Henriquez CS. Simulating the electrical behavior of cardiac tissue using the bidomain model. Crit Rev Biomed Eng. 1993; 21:1–77. [PubMed: 8365198]
47. Roth BJ. How the anisotropy of the intracellular and extracellular conductivities influences stimulation of cardiac muscle. J Math Biol. 1992; 30:633–46. [PubMed: 1640183]
48. Rane AA, Chuang JS, Shah A, Hu DP, Dalton ND, Gu Y, et al. Increased Infarct Wall Thickness by a Bio-Inert Material Is Insufficient to Prevent Negative Left Ventricular Remodeling after Myocardial Infarction. PLoS ONE. 2011; 6:e21571. [PubMed: 21731777]
49. Sabbah HN, Wang M, Gupta RC, Rastogi S, Ilsar I, Sabbah MS, et al. Augmentation of Left Ventricular Wall Thickness With Alginate Hydrogel Implants Improves Left Ventricular Function and Prevents Progressive Remodeling in Dogs With Chronic Heart Failure. JACC: Heart Failure. 2013; 1:252–8. [PubMed: 23998003]
50. Mukherjee R, Zavadzkas JA, Saunders SM, McLean JE, Jeffords LB, Beck C, et al. Targeted myocardial microinjections of a biocomposite material reduces infarct expansion in pigs. Ann Thorac Surg. 2008; 86:1268–76. [PubMed: 18805174]
51. Suarez S, Almutairi A, Christman KL. Micro- and Nanoparticles for Treating Cardiovascular Disease. Biomaterials Science. 2015; 3:564–80. [PubMed: 26146548]

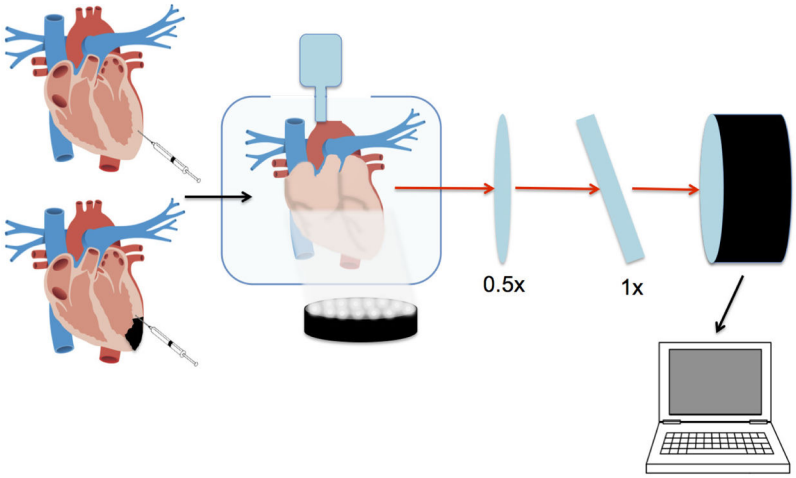

Fig. 1.

Schematic of experimental procedure. The healthy and cryoinfarcted hearts injected with the hydrogel or saline are depicted, followed by the optical mapping setup. The heart is excised and the aorta is cannulated for perfusion of the tissue with Tyrodes solution, allowing the heart to remain viable *ex vivo*. A voltage sensitive dye (di-4-ANNEPS) is perfused through the coronaries. A LED light excites the dye at 470 nm (black arrow) and the emitted fluorescence is collected at a wavelength greater than 610 nm (red arrows). The incident fluorescent signal is captured by a high-speed camera (1000 frames/second) and then computational techniques are used to analyze the data.

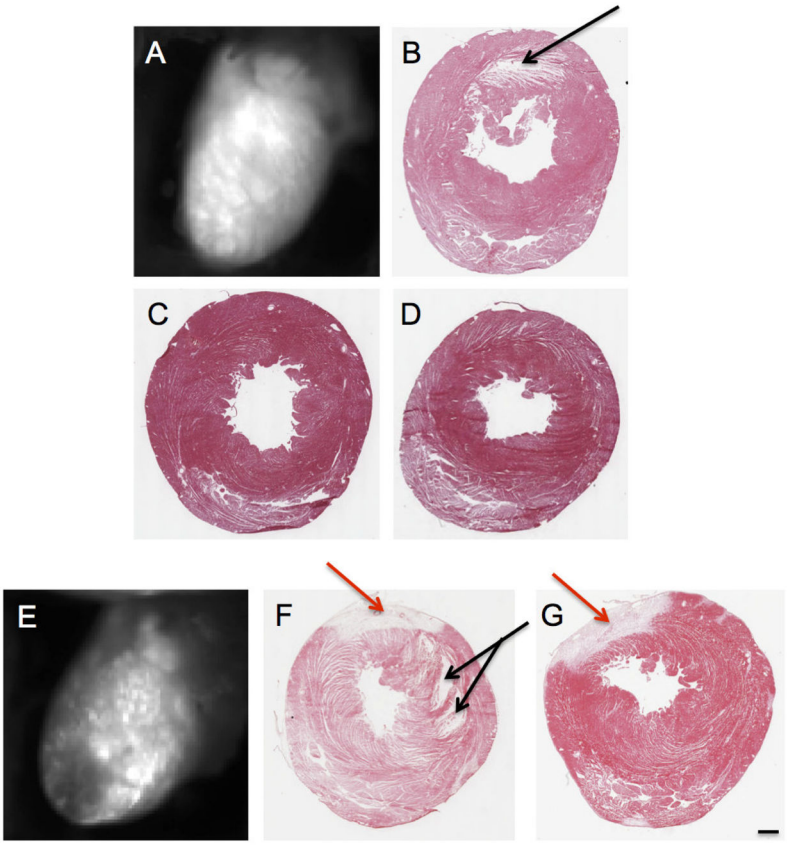

Fig. 2.

Histological analysis. (A) Representative fluorescent image of the di-4-ANNEPS-perfused healthy heart. Note: dye perfusion over the entire epicardial surface. Representative slides stained with H&E for histological assessment of (B) hydrogel-injection (C) no-injection (D) and saline-injection after optical mapping. A black arrow denotes the hydrogel in the myocardium. All photomicrographs are taken at 1X and scale bar is 1mm. (E) Representative fluorescent image of the di-4-ANNEPS perfused cryoinfarcted heart. Note: dye perfusion over the entire epicardial surface except the cryoinfarct. Representative slides stained with H&E for histological assessment of (F) hydrogel-injection (G) and no-injection after optical mapping. Red arrows denote the cryoinfarction.

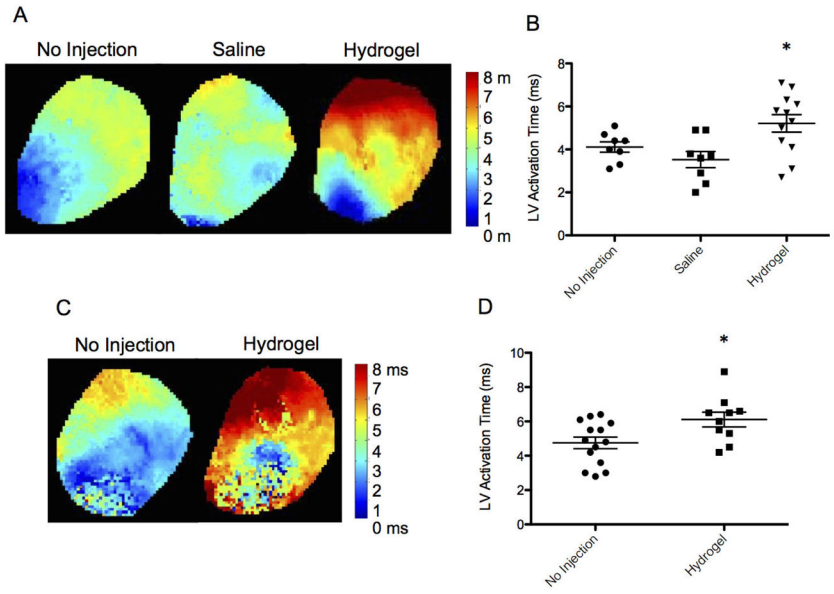

Fig. 3.

LV activation time. (A) Representative activation maps of the LV free wall of healthy hearts demonstrate high LV activation time at the base in the hydrogel injected group indicating slowed action potential propagation when compared with saline and no-injection. (B) Total LV activation time was significantly greater in the hydrogel injected group compared to all other groups (*$p < 0.01$). (C) High LV activation time was also visible in cryoinfarcted hearts injected with a hydrogel compared to no-injection. (D) Moreover, total LV activation time was significantly greater in cryoinfarcted hearts in the hydrogel group compared to no-injection (*$p < 0.02$).

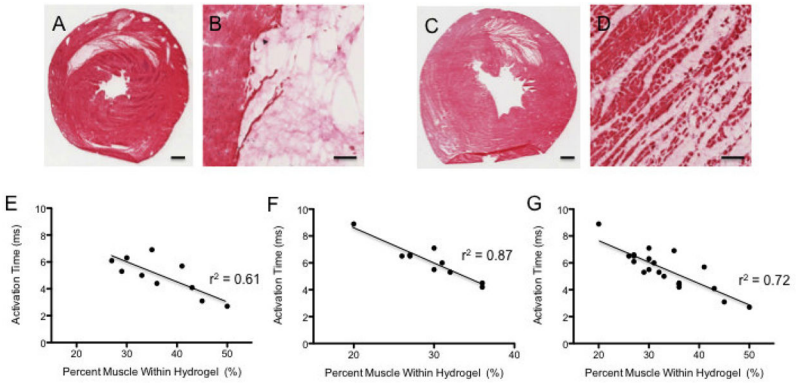

Fig. 4.

Hydrogel interstitial spread. Representative images of myocardium injected with hydrogels exhibiting (A–B) low and (C–D) high interstitial spread. Hearts with an average of 27% and 50% percent muscle within the hydrogel are shown in A and C, respectively. Increased percent muscle within the hydrogel resulted in lower activation time in both (E) healthy ($r = -0.78$; $p < 0.008$) and (F) cryoinfarcted ($r = -0.93$; $p < 0.0001$) hearts. (G) The percent muscle within the hydrogel ranged from 20–50% across all hearts ($r = -0.85$; $p < 0.0001$). Scale bar: 1mm (A & C); 100 μm (B & D).

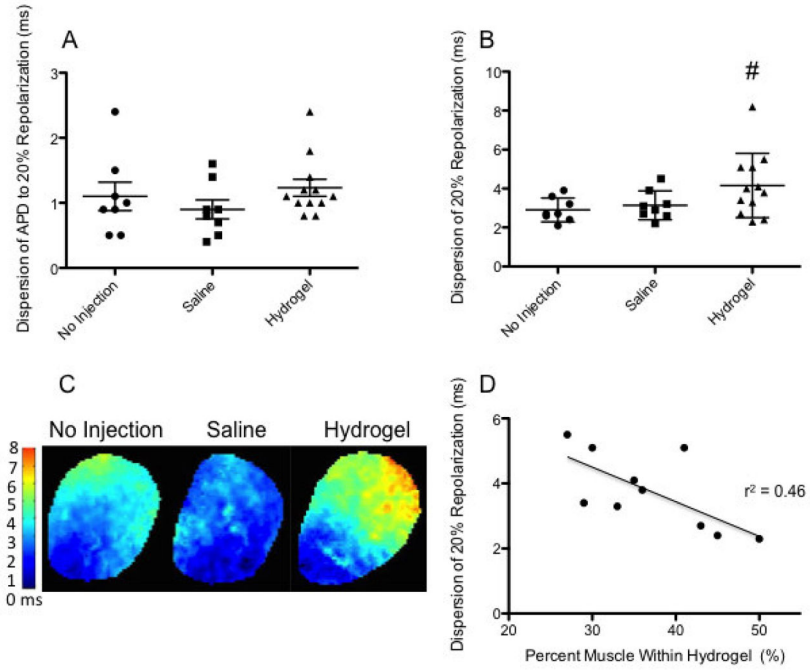

Fig. 5.

Dispersion of APD and repolarization. (A) Dispersion of APD at 20% repolarization revealed no significant differences between groups in healthy hearts. (B) While more variability was visible in 20% repolarization values in hydrogel-injected hearts compared to no-injection and saline-injection, differences were not significant (#p = 0.06) (C) Color maps depicting the time of 20% repolarization at each pixel of the LV free wall show slightly greater dispersion in hydrogel-injected hearts. (D) The increased dispersion in 20% repolarization times correlated significantly with the percent muscle in the hydrogel ($r = -0.67$; $p < 0.03$).

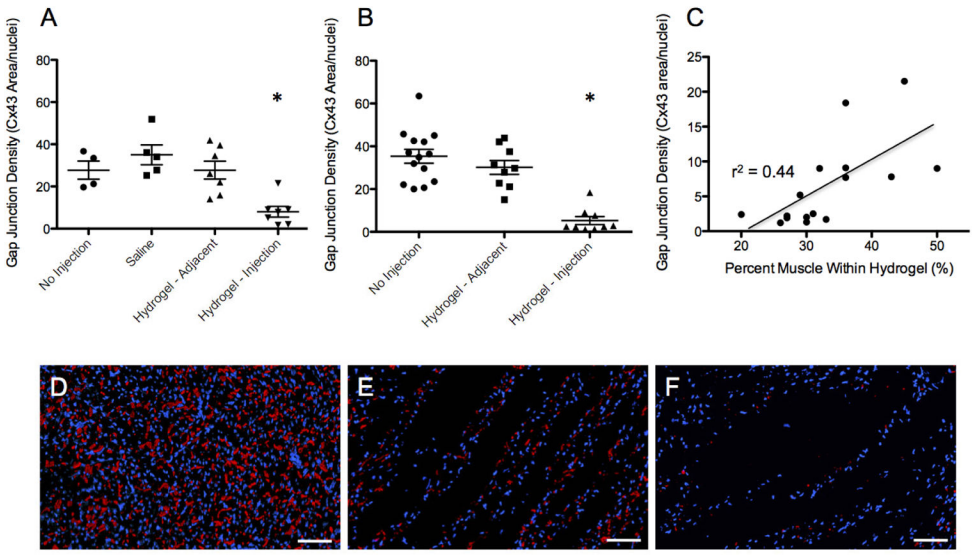

Fig. 6.

Gap junction density. (A) Gap junction densities (Cx43+ area (μm^2)/number of nuclei) within the hydrogel injection site of (A) healthy (*$p < 0.0005$) and (B) cryoinfarcted (*$p < 0.0001$) were significantly lower than all other groups. Density of gap junctions was normalized to cell number to take into account blank regions containing the hydrogel. (C) Increased percent muscle within the hydrogel in healthy and cryoinfarcted hearts resulted in increased gap junction density ($r = 0.66$; $p < 0.005$). Representative images of (D) non-injected, (E) highly spread hydrogel-injected and (F) minimally spread hydrogel-injected hearts display the variability in gap junction (red) density. Scale bar: 100 μm.

Table 1

Hemodynamic data.

	Baseline		Post-injection	
	EDP (mmHg)	**PSP (mmHg)**	**EDP (mmHg)**	**PSP (mmHg)**
None - Healthy	9.03 ± 0.47	99.87 ± 3.40	8.37± 0.45	81.27 ± 4.45
Saline - Healthy	7.96 ± 0.34	95.35 ± 2.16	8.06± 0.45	74.50 ± 5.39
Hydrogel - Healthy	8.05 ± 0.41	91.10 ± 9.15	8.57± 0.45	73.88 ± 8.23
None - Cryoinfarct	8.16 ± 0.31	95.94 ± 3.16	7.94± 0.37	95.82 ± 3.09
Hydrogel – Cryoinfarct	8.34 ± 0.29	97.82 ± 2.44	8.38± 0.35	82.06 ± 5.04

Table 2

Action potential duration data.

	APD20	APD50	APD80
None - Healthy	11.9 ± 0.3	22.1 ± 0.8	47.9 ± 1.5
Saline - Healthy	11.2 ± 0.3	20.5 ± 0.6	45.1 ± 1.6
Hydrogel - Healthy	11.9 ± 0.2	22.2 ± 0.5	48.0 ± 1.2
None - Cryoinfarct	13.7 ± 0.4	26.8 ± 1.0	54.3 ± 1.8
Hydrogel - Cryoinfarct	15.1 ± 0.4	30.2 ± 1.0	57.6 ± 1.4